

Research on the Vortex-induced Vibration of A Cylinder Under Oscillatory Flow

Di Peng^{1,*}, Longda Zhou

¹Peking University, Beijing 100871, China

²Nanchang Innovation Institute of Peking University, Nanchang 330096, China

*Corresponding author

Abstract: Riser system is an indispensable structure connecting offshore platform and submarine wellhead, which is very common in offshore engineering. When the fluid flows through the riser system, the vortex falls off on both sides of the riser and stimulates the riser vibration, resulting in the fatigue damage of the riser. The vortex-induced vibration under oscillating flow is analyzed in this paper. The results show that the vortex-induced vibration of cylindrical structures in oscillating flow is more regular when the reduced velocity is low. The oscillating flow causes multi-mode vibration of the cylindrical structure, and the locking interval increases with the increase of KC number. The shed vortices will pass through the cylinder again after changing the flow direction, changing the fluid force on the cylinder structure.

Keywords: Oscillatory flow; Vortex-induced vibration(VIV); Fluid-structure interaction; RANS Model.

1. Introduction

Riser system is an essential part of offshore oil extraction, and it is a key component connecting subsea equipment and floating platforms. The fluid flows through the object and forms a regular combination of staggered vortices behind the structure, called Karman vortex streets. When the cylindrical structure of the elastic support riser is placed in the incoming flow at a certain speed, the two sides of the cylinder will produce alternating decreasing vorticity, and the cylinder will be affected by the hydrodynamic pressure of the incoming flow direction and the vertical incoming flow, which will cause the cylinder vibration. In turn, the vibration of the cylinder affects the cascade form of the wake, and this interaction between the fluid and the structure is called vortex-induced vibration. Its mechanism and vibration characteristics have been extensively studied for a long time [1-4].

The existing numerical models can be generally divided into frequency-domain and time-domain methods[5]. Frequency domain forecasting tools based on semi-empirical models have been well developed, such as SHEAR7[6] and VIVANA[7]. Empirical models are highly dependent on empirical parameters [8]. Aronsen[9] measured the fluid force of a rigid cylinder in pure down-flow vibration, and drew the cloud map of the fluid force coefficient. Through the rigid cylindrical VIV experiment, Yin et al. [10] show that when CF and IL vibrate at the same time, IL fluid force coefficient increases significantly. Sanaati et al. [11] measured the fluid force coefficient of a flexible cylinder VIV and studied the relationship between the pulsation resistance coefficient and the axial force. Tang Guoqiang [12] used the finite element method to identify the fluid force coefficient of flexible cylinder VIV and showed that the magnitude of IL fluid force coefficient is related to the phase difference between force and displacement. Song et al. [13] inversely solved the fluid force of a flexible cylinder VIV, and found that the pulsation resistance coefficient was closely related to IL displacement and frequency, and was significantly different from that of a rigid cylinder. The additional mass coefficient was not evenly

distributed along the axial direction of the cylinder, and abrupt changes appeared at the displacement nodes. In this paper, the vortex-induced vibration of oscillating flow with KC numbers of 25 and 50 is studied.

2. Numerical Calculation Model and

2.1. Governing equations

In this paper, unsteady incompressible RANS governing equation is used to simulate the flow field of the calculated basin. When considering the changes brought about by the movement of the cylinder, the RANS equation is:

$$\frac{\partial U_i}{\partial x_i} = 0 \quad (1)$$

$$\frac{\partial U_i}{\partial t} + C_j \frac{\partial U_i}{\partial t} = -\frac{1}{\rho} \frac{\partial P}{\partial x_i} + \frac{\partial}{\partial x_j} (2\nu S_{ij} - \overline{u'_i u'_j}) \quad (2)$$

where, U_i represents the magnitude of the fluid motion velocity, x_i is the fluid particle coordinates, ρ is the fluid density, is the motion viscosity coefficient, P is the pressure, U_j is the mesh motion velocity, $C_j = U_i - U_j$ is the velocity of the fluid relative to the mesh. S_{ij} , $-\overline{u'_i u'_j}$ is the average strain tensor and the Reynolds stress term, namely the turbulence effect, respectively expressed as:

$$S_{ij} = \frac{1}{2} \left(\frac{\partial U_i}{\partial x_j} + \frac{\partial U_j}{\partial x_i} \right), \quad -\overline{u'_i u'_j} = 2\nu_t S_{ij} - \frac{2}{3} \delta_{ij} k \quad (3)$$

ν_t is the turbulent viscosity coefficient, k is the turbulent kinetic energy, δ_{ij} is the Kronecker symbol.

The equation of motion of the cylindrical structure is:

$$m\ddot{y}(t) + c\dot{y}(t) + ky(t) = F_y(t) \quad (4)$$

y is the vibration displacement of the cylindrical structure, m , c and k are the mass, structural damping and spring stiffness of the structure respectively, and F_y is the force perpendicular to the flow direction of the structure.

2.2. Computational model

The computational model adopted in this paper is shown in Figure 1. The cylindrical structure is in the center of the calculated basin of the model. The diameter of the cylindrical structure is D , and the calculated basin length is $80D$ and width is $25D$. It is set that simple harmonic motion occurs on the left and right edges of the two ends of the model to drive the fluid in the model to generate oscillating flow. By controlling different simple harmonic motion on the model boundary, the cylinder structure is placed in different flow conditions. Then, the vortex-induced vibration response characteristics of the structure under different conditions are compared and analyzed. There are three velocity monitoring points A, B and C in the basin. By observing the velocity changes of the three points, we can analyze whether the boundary motion can produce effective oscillating flow. The velocity of the boundary movement at both ends of the model is equal and in the same direction. The velocity expression is as follows:

$$U(t) = U_m \cos(2\pi f_{os} t) \quad (5)$$

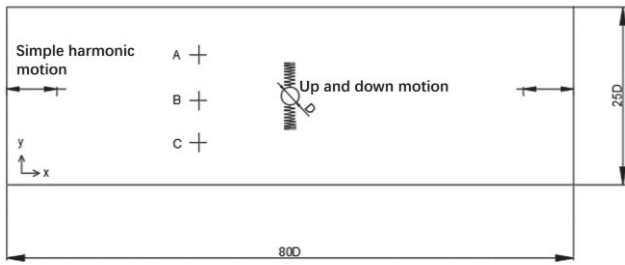


Figure 1. Computational domain

where, $U(t)$ represents the instantaneous speed of the boundary at both ends of the model, U_m is the maximum speed of the boundary movement at both ends of the model, f_{os} represents the round-trip frequency, and t is the time. Generally, the dimensionless parameter KC number is used to analyze the effect of oscillating flow on vortex-induced vibration of structures under different conditions. KC number is defined as: $KC = U_m / (f_{os} D)$.

Part of the calculated grid is shown in Figure 2. A total of 200 grid nodes are set on the surface of the cylindrical structure, and the thickness of the boundary layer is $0.001D$.

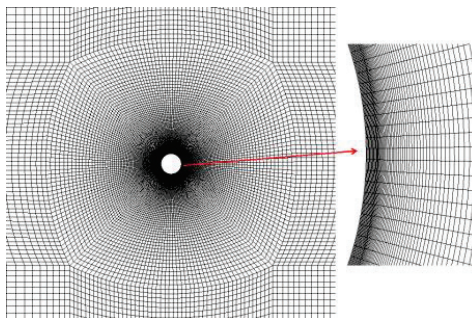


Figure 2. Mesh details

3. Numerical Calculation Model and Verification

The displacement curves with reduced velocities of 2 to 15 corresponding to KC numbers of 25 and 50 were fitted in the same coordinate system, as shown in Figure 3.

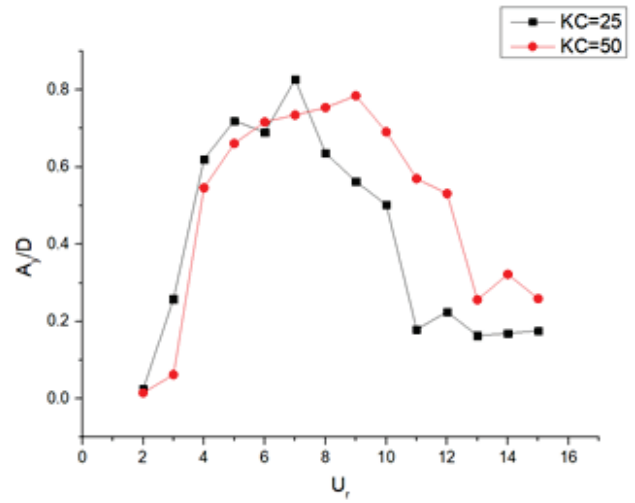


Figure 3. Amplitude ratio at different reduced speeds of KC=25 and KC = 50

It is found that the number of KC has little effect on the amplitude, which is about $0.8D$ in both cases. A KC number of 25 corresponds to a locking interval of 4 to 10, and a KC number of 50 corresponds to a locking interval of 4 to 12. As the number of KC increases, the locking range becomes larger. Under the condition that the KC number is 25 and the reduced velocity is 5, 8 and 15, the displacement time curve obtained is shown in Figure 4. According to the images, when the reduced velocity is 5 and 8, the vibration of the structure is more regular, the upper and lower vibration is symmetrical, the amplitude is roughly equal, and the displacement time curve of the two cases does not change much. When the reduced velocity increases to 15, the displacement time curve changes obviously, the amplitude decreases significantly, and the vibration is asymmetrical, the lower end corresponds to a larger amplitude, and the upper end of the displacement curve appears a secondary peak.

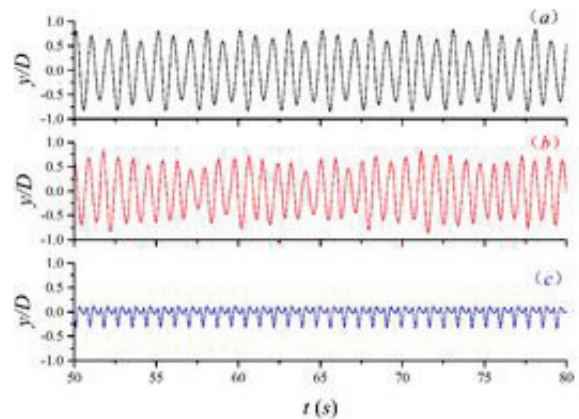


Figure 4. Displacement history curve of KC=25 cylinder in y direction: (a) $U_r=5$, (b) $U_r=8$, (c) $U_r=15$

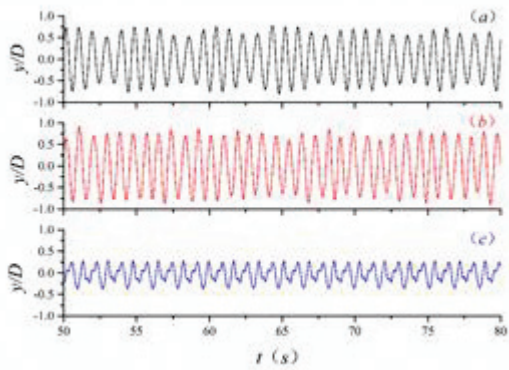


Figure 5. Displacement history curve of KC=50 cylinder in y direction: (a) $U_r=5$, (b) $U_r=8$, (c) $U_r=15$

Under the condition that the KC number is 50 and the reduced velocity is 5, 8 and 15, the displacement time curve obtained is shown in Figure 5. When the reduced velocity is 5 and 8, the displacement time curve is like that when the KC number is 25, and the amplitude changes little. When the reduced speed increases to 15, there are two peaks of amplitude in both the upper and lower directions, and the upper and lower vibration amplitudes are roughly equal. The results of the two experiments show that the vortex-induced vibration of the cylindrical structure in the oscillating flow is more regular when the reduced velocity is low, and the amplitude up and down is roughly equal.

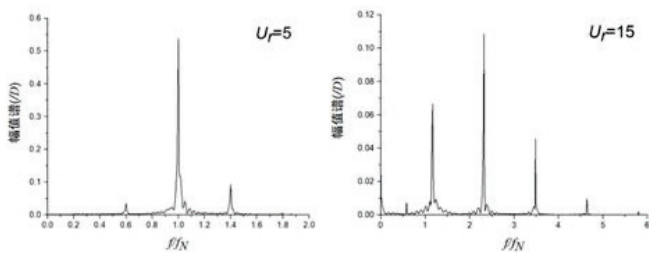


Figure 6. Spectrum diagram at different reduced velocities of KC=25

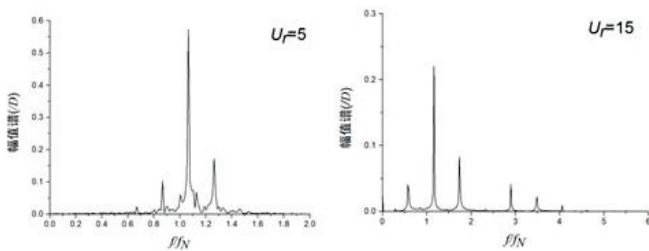


Figure 7. Spectrum diagram at different reduced velocities at KC=50

The displacement time curves with KC number of 25 and 50 and reduced velocity of 5 and 15 respectively are converted to obtain the spectrum diagram shown in Figure 6 and 7 (because the displacement time curves with reduced velocity of 5 and 8 are similar, only the case with reduced velocity of 5 is selected for consideration here). When the KC number is 25 and the reduced speed is 5, the vibration is mainly fixed at 1 frequency. When the reduced speed increases to 15, the number of excitation frequencies

increases and the multi-mode vibration becomes obvious. When the KC number is 50 and the reduced speed is 5, the vibration frequency is mainly fixed at 1.06 times the natural frequency, and when the reduced speed increases to 15, the number of dominant frequencies also increases. The oscillating flow will cause multi-mode vibration of the cylindrical structure.

The experimental results obtained in this paper are compared with the experimental results of Sumer[14] and the numerical results simulated by Zhao[15], etc. The experimental results in this paper basically fit the other two results. The locking region obtained in this paper is 4 to 7, the numerical result of Zhao et al simulation is also 4 to 7, and the experimental result of Sumer is 5 to 7. Compared with the experimental result, the locking region obtained by numerical simulation is too large. As shown in Figure 8, it is the isogram of vorticity change at four similar moments when the KC number is 25 and the reduced velocity is 5. Figure 9 shows the curves of fluid velocity and structural force, displacement, and time under the same conditions. According to the diagram, whenever the fluid flow rate passes the peak, the force curve of the structure in the lag area will fluctuate, and the corresponding relationship is shown in region A in Figure 9.

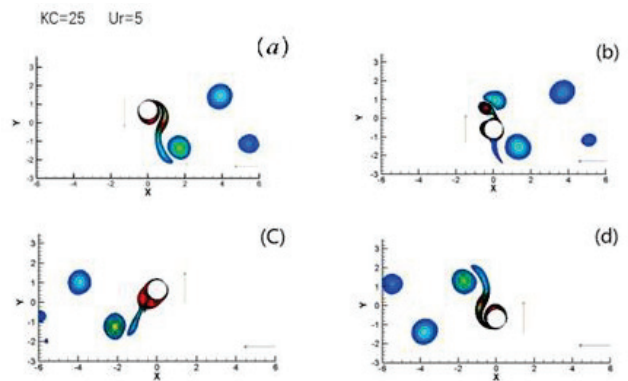


Figure 8. Contour map of vorticity change: (a) $t=81.1s$ (b) $t=81.6s$ (c) $t=83s$ (d) $t=83.6s$

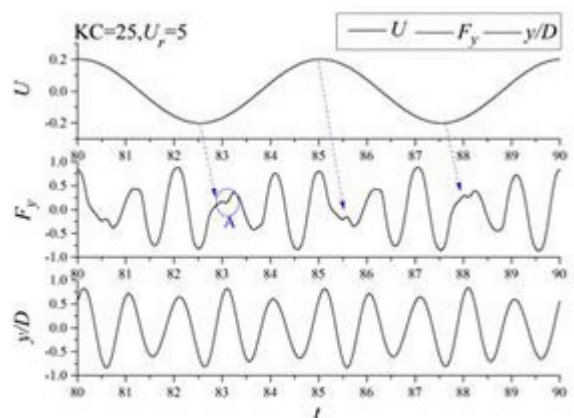


Figure 9. Velocity of oscillation and displacement curve of cylinder y direction at different time

In Figure 8, (a) and (b) correspond to the peak of the fluid force around $t=81.6s$ and $82.08s$, and observe the image, combined with the velocity time curve, at this time, the dropped vortices in the previous cycle pass through the cylindrical structure again, passing above and below the

structure respectively, so that the peak value appears on the stress curve. When the vortex generated in the previous cycle completely passes through the structure, the force of the structure is completely from the force generated by the vortex shedding in the current cycle, so the secondary peak value corresponding to the stress curve in region A is smaller than that of the peak value.

4. Conclusion

The vortex-induced vibration of structures with KC numbers of 25 and 50 is analyzed in this paper. The conclusion is as follows: When the reduced velocity is low, the vortex-induced vibration of the cylindrical structure in the oscillating flow is more regular. In addition, it is found that the oscillating flow causes multi-mode vibration of the cylindrical structure, and the locking interval increases with the increase of KC number. The shed vortices will pass through the cylinder again after changing the flow direction, changing the fluid force on the cylinder structure.

References

- [1] Sarpkaya, T. (2004). A critical review of the intrinsic nature of vortex- induced vibrations. *Journal of Fluids and Structures*, 19(4): 389-447.
- [2] Williamson, C.H.K., Govardhan, R. (2008). A brief review of recent results in vortex- induced vibrations. *Journal of Wind Engineering and Industrial Aerodynamics*, 96(6/7): 713-735.
- [3] Xu, W.H., Ma, Y.X., Luo H., et al. (2017). Vortex-induced vibration of an inclined flexible cylinder with a small yaw angle. *Journal of Harbin Engineering University*, 38(2): 195-200.
- [4] Ji, C.N., Xing, G.Y., Zhang, L.,et al. (2018). Numerical simulations of vortex-induced vibration of flexible riser subjected to inclined flow. *Journal of Harbin Engineering University*, 39(2): 324-331.
- [5] Yuan,Y.C., Xue,H.X., Tang,W.Y. (2018).Vortex-induced vibration time domain responses of flexible risers under oscillatory flows. *Journal of Vibration and Shock*, 37(13): 56-64.
- [6] Andiver, J. K., Li, L.S. (2005). 4 program theoretical manual. Cambridge, MH: Massachusetts Institute of Technology.
- [7] Arsen, C. M., Lie, H, Passano, E., et al. (2009). VIVANA theory manual(version3. 7). Trondheim, Norway: Norwegian Marine Technology Research Institute.
- [8] Xu, W.H., Ma, Y.X., Zhang, S.H., et al. (2018). Analysis on response and fluid force characteristics of a cylinder subjected to vortex-induced vibration in flow direction. *Journal of Harbin Engineering University*, 39(12): 1902-1909.
- [9] Aronsen, K. H. (2007). An experimental investigation of in-line and combined in-line and cross-flow vortex induced vibrations. Trondheim: Norwegian University of Science and Technology.
- [10] Yin, D.C., Larsen, C. M. (2010). On determination of VIV coefficients under shear flow condition. *Proceedings of the ASME 2010 29th International Conference on Ocean, Offshore and Arctic Engineering*. Shanghai, 547-556.
- [11] Sanaati, B., Kato, N. (2013). Vortex-induced vibration (VIV) dynamics of a tensioned flexible cylinder subjected to uniform cross-flow. *Journal of marine science and technology*, 18(2): 247-261.
- [12] Ji, N.S., Lin, L., Bin, T. et al. (2011). Laboratory tests of vortex-induced vibrations of a long flexible riser pipe subjected to uniform flow. *Ocean Engineering*, 38(11-12):1308-1322.
- [13] Song, L.J., Fu, S.X., Cao J., et al. (2016). An investigation in to the hydrodynamics of a flexible riser undergoing vortex-induced vibration. *Journal of Fluids and Structures*, 63: 325-350.
- [14] Sumer, B.M., Fredsoe, J. (1988). Transverse vibrations of an elastically mounted cylinder exposed to an oscillating flow. *Journal of Offshore Mechanics and Arctic Engineering*. 110:387-394.
- [15] Zhao, M., Cheng, L., An, H. (2012). Numerical investigation of vortex-induced vibration of a circular cylinder in transverse direction in oscillatory flow. *Ocean Engineering*, 41: 39-52.